Crystal-field splitting of core excitons in ionic crystals

F. Sette, B. Sinkovic, Y. J. Ma, and C. T. Chen
AT&T Bell Laboratories, Murray Hill, New Jersey 07974
(Received 27 December 1988)

High-resolution and temperature-dependent photoabsorption measurements at the potassium $L_{2,3}$ edges in KF, KCl, KBr, KI, and $KMnF_3$ are used to study the crystal-field splitting of potassium $2p^{-1}3d$ core excitons. The direct observation of two split states allows one to explore the dependence of the crystal-field potential and of the $3d$ orbital spatial extent on thermal expansion, atomic vibrational motion, and the halide atom. Using the simple $10Dq$ theoretical model, we measured the size of the $3d$ orbitals and found that they collapse toward the potassium $2p$ core hole. The dynamical character of this process is demonstrated by the correlation between the core-exciton size and the optical dielectric constant.

I. INTRODUCTION

Empty or partially empty d states in cubic ionic crystals are no longer degenerate. This energy-level splitting is induced by the crystal-field potential. A simple description of this effect is given by the $10Dq$ crystal-field theory[1,2] in which the crystal-field potential is determined by point charges at the positions of the atoms in the lattice. In crystals with cubic symmetry, this potential splits the d orbitals into two states belonging to the E_g and T_{2g} representations. Photoabsorption studies involving excitations of these two levels have been widely used to determine the crystal-field splitting Δ, and to study how the crystal-field potential depends on interatomic distances, charge distribution, vibrational amplitudes, and the ionic material.[2] Most of the previous work was performed on transition-metal compounds, by monitoring the quadrupole-allowed d-to-d optical transitions between filled and empty crystal-field-split states.[2] Dipole-allowed excitations from highly dispersive p-like valence bands or shallow p core levels were used to probe these split states in materials with unfilled d orbitals. In these studies, however, it was difficult to interpret the data because of the complicated coupling between the various unoccupied states.[3,4]

We present a study on potassium halides and $KMnF_3$ where properties of the crystal-field-split potassium $3d$ empty states are derived from photoabsorption measurements of the potassium $L_{2,3}$ edges. As a consequence of the $2p$ core hole being highly localized on the potassium atom, the $2p^{-1}3d$ excitation has a strong core-excitonic character and can be observed as a sharp resonance in the core photoabsorption spectrum.[5,6] We studied how the crystal-field potential splits this $2p^{-1}3d$ resonance by monitoring changes of the absorption spectra as a function of halide atom, crystal structure, and sample temperature. We identify the crystal-field-split states, and we show that they can be conveniently probed with the present technique. Our data compare very well with the predictions of the simple $10Dq$ theoretical model, and indicate that the spatial extent of the potassium $3d$ orbitals depends on halide ion and on lattice size. The latter observation can be explained by the dynamical screening of the $2p$ hole.

II. EXPERIMENT

The potassium $L_{2,3}$ edge photoabsorption spectra of KF, KCl, KBr, KI, and $KMnF_3$ were measured using total-electron-yield detection. The KCl, KBr, and $KMnF_3$ samples were single crystals. KF and KI were high-purity crystalline powders. The highly reactive KF powder was deposited on a metal substrate and held with a fine copper mesh (40 lines/cm). Previous attempts using methanol or other vacuum compatible adhesives resulted in absorption spectra with broader features and reduced crystal-field splitting, indicating chemical reaction of the KF compound. The samples were exposed to a total soft-x-ray radiation of 10^{12} photons/mm^2 in order to accumulate a spectrum. No photon damaging was observed in the data presented here. The experiments were performed using the newly constructed AT&T Bell Laboratories "Dragon" soft-x-ray beam line located on the VUV synchrotron storage ring at Brookhaven National Laboratory. This instrument, the spherical version of the cylindrical elements monochromator theoretical design, was operated with energy resolution 30 meV.[7,8]

III. RESULTS AND DISCUSSION

In Fig. 1 we report the 300-K photoabsorption data of the five crystals. The potassium halide spectra show two well-resolved peaks A,B, and $A,'B,'$ for each $2p$ spin-orbit-split component, $2p_{3/2}$ and $2p_{1/2}$,[5,6] but only one peak is observed for each edge in the spectrum of $KMnF_3$. These features are due to excitations of the $2p$ core electron into the potassium $3d$ empty orbitals. The weak preedge shoulders, seen in all our samples, are likely to be associated with transitions into empty states derived from the potassium $4s$ orbitals. These shoulders will not be further discussed in the present paper.

In the following we will use the simple $10Dq$ theory to demonstrate that the two features observed in the potassium halides, peaks A and B (A' and B'), are electronic

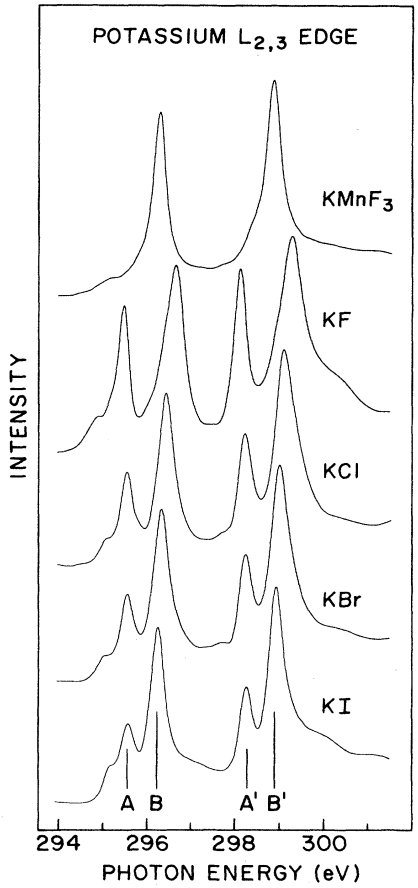

FIG. 1. Potassium $L_{2,3}$-edge photoabsorption spectra taken at 300 K on $KMnF_3$, KF, KCl, KBr, and KI. Peaks A and B (A' and B') are the excitations from the $2p_{3/2}$ ($2p_{1/2}$) core level to the crystal-field-split $3d$ states. The energy scale refers to the KCl spectrum. The other spectra have been arbitrarily shifted to help visualize changes in the crystal-field splitting.

transitions from the $2p$ levels to the T_{2g} and E_g crystal-field-split $3d$ states.[2] The presence of Mn^{2+} ions in the K^+ second shell, however, renders the splitting Δ unmeasurable in $KMnF_3$.

The $10Dq$ crystal-field theory considers the potential arising from point charges being localized in the positions of the atoms in the crystal. This approach is generally valid in ionic compounds.[2] The crystal-field potential, V_n, due to point charges having cubic symmetry and belonging to the nth shell of the potassium ion, can be expressed around the potassium as[2]

$$V_n = V_{0n} + D_n(x^4+y^4+z^4-\tfrac{3}{5}r^4)+\cdots , \quad (1)$$

where the ellipsis indicates higher-order terms, and D_n is a geometrical factor depending upon the position, charge, and number of ions in the nth shell. V_{0n} is the constant term in the potential. For the nth shell, D_n is given by

$$D_n = \frac{35C_nZe^2}{4a_n^5} , \quad (2)$$

where a_n is the distance from the potassium, Ze is the charge on each atom, and the constant C_n is determined by the number and position of the atoms. For example, in KF, where there are six fluorine atoms around the potassium, C_1 is equal to -1. In $KMnF_3$ there are 12 fluorine atoms and C_1 is equal to 0.5. The total crystal-field splitting Δ of the d orbitals is given by

$$\Delta = 10Dq . \quad (3)$$

D is the summation of the D_n factors from all the coordination shells. The quantity $q = 2\langle r^4\rangle_{3d}/105$ is determined by the quantum average of the operator r^4 over the potassium $3d$ wave functions. The separation Δ results from the energy shift of the T_{2g} and E_g states being displaced, respectively, by $-4Dq$ and $+6Dq$ from their unsplit position. The relative energy position of the T_{2g} and E_g levels is defined by the sign of D.

The a_n^{-5} dependence of D_n in Eq. (3) implies that the splitting is most sensitive to the ions constituting the first-neighbor shell. For this reason, and for the different geometric factors C_1, the absolute value of Δ should be approximately 2 times larger in KF than in $KMnF_3$, and the two crystal-field-split doublets should be observed in both samples. The contradictory results of Fig. 1 are explained by considering higher coordination shells. In Table I we list the D_n values and their accumulated values, D_n^T, for the first five shells of KF and $KMnF_3$. The total D values are also given. All these quantities, expressed in units of D_1, were calculated using Eq. (2) for the two crystal structures. We observe that in KF D_1 is already very close to the final value D. On the other hand, in $KMnF_3$ the eight Mn^{2+} ions in the second shell give a D_2 comparable and opposite in sign to D_1. Similar important contributions also come from the other listed shells. The special charge arrangement in $KMnF_3$ is

TABLE I. D values for different shells around a K^+ ion in KF and $KMnF_3$.

Shell	KF				$KMnF_3$			
n	Ions		D_n/D_1	D_n^T/D_1	Ions		D_n/D_1	D_n^T/D_1
1	6	F^-	1.000	1.000	12	F^-	1.000	1.000
2	12	K^+	0.088	1.088	8	Mn^{+2}	−1.290	−0.290
3	8	F^-	−0.057	1.031	6	K^+	0.353	0.063
4	6	K^+	−0.031	1.000	24	F^-	0.129	0.192
5	24	F^-	0.014	1.014	12	K^+	−0.032	0.160
∞				1.022				0.133

therefore responsible for the very small value of D. If we assume similar values for the quantum average q in KF and $KMnF_3$, the absolute value of the crystal-field splitting is, in fact, reduced by a factor of 0.06, i.e., the observed values of $\Delta \simeq 1$ eV for the potassium halides are reduced to $\Delta \simeq 60$ meV for $KMnF_3$. Since the intrinsic linewidth of the potassium $2p$ core hole is ~ 0.2 eV, such a small splitting cannot be observed in the $KMnF_3$ spectrum. These simple arguments enforce our peaks assignment as due to excitation into crystal-field-split $3d$ orbitals[9] and allows for a *direct* determination of the splitting Δ from the energy separation of peaks A and B (A' and B').

In the following we will examine the dependence of the crystal-field splitting from the lattice constant of the different potassium halides. Table II summarizes the photoabsorption energy position of the various peaks in Fig. 1, and the experimental values of Δ obtained from the energy separations between peaks A and B, and peaks A' and B' in the potassium halide samples. Interestingly, these values are approximately half of those derived from $3p3d^{-1}$ shallow core-exciton measurements,[4] and agree well with previous measurements of the potassium $L_{2,3}$ edges.[6] We will show that this difference can be explained by the more localized character of the $2p$ hole. Table II also lists the potassium halide bond distances a_1. The expected trend of Δ increasing with decreasing bond distance is clearly observed. A more illustrative analysis can be done by plotting the logarithm of Δ as a function of the logarithm of a_1. According to the $10Dq$ theory and Eq. (2), the relation between these two quantities is linear with a slope of -5. As seen in Fig. 2, the solid dots, representing our measured values, do not follow the solid line, representing the predicted relation, but show a variation with a smaller decreasing rate. This behavior may indicate that, within the $10Dq$ theory, differences in chemical bonding and lattice size change the value of q, i.e., the spatial extent of the unoccupied potassium $3d$ wave functions [see Eq. (3)].

A study of the crystal-field splitting as a function of temperature, in the same potassium halide, allows one to derive the detailed dependence of Δ on lattice size without involving differences in chemical bonding. Figure 3 shows the potassium $L_{2,3}$ absorption spectra of KCl

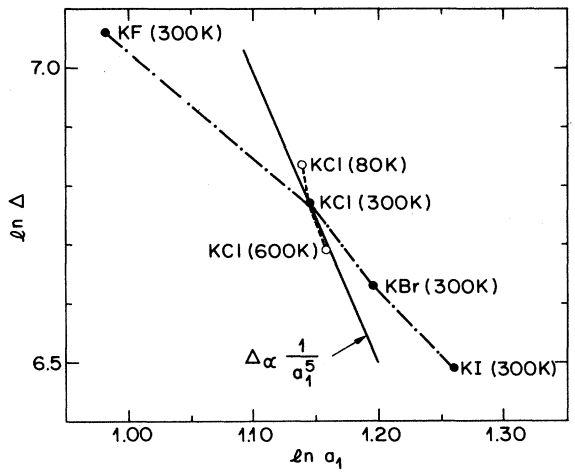

FIG. 2. Relation between crystal-field splitting Δ and potassium halide bond distance a_1. Values for KF, KCl, KBr, and KI measured at 300 K are shown by the solid dots, linked by a dotted-dashed line. Values for KCl at 80 and 600 K are shown by the open circles, linked by a dashed line through the 300-K value. The a_1^{-5} dependence of Eq. (2) is also shown by the solid line.

taken at sample temperatures of 80, 300, and 600 K. It can be seen that with increasing sample temperature the energy positions of peaks A and B, as well as peaks A' and B', shift toward each other, and the linewidths of all the peaks are greatly increased. These features are determined by the lattice thermal expansion and the atomic vibrational motion. We will discuss the peak shifts first, and then the broadening of the linewidth.

At the higher temperatures the lattice thermal expansion increases the potassium-halide distance, and this, reducing the crystal-field splitting Δ, explains the peak shifts. Table III(a) lists the absolute energy of peaks A, B, A', and B'. The splittings and the bond distances are also given.[10] The temperature-dependent full width at half maximum values of KCl are reported in Table III(b). The increase in linewidths is as large as 250 meV. This unusual broadening is caused by the fact that the photoabsorption process is much faster than the atomic motion, so that the crystal-field potential experienced by

TABLE II. Summary of the photoabsorption energies for peaks A, B, A', B', of the crystal-field splitting Δ and of the first-neighbor bond distance a_1 in the potassium halides and $KMnF_3$ samples. The accuracy for our energy calibration is ± 50 meV. The precision between peaks of different spectra is ± 20 meV while it is better than ± 10 meV for peaks in the same spectrum. Δ is calculated by averaging the separations between peaks A, B and that of A', B'.

	A (eV)	B (eV)	A' (eV)	B' (eV)	Δ (meV)	a_1 (Å)
KF	295.671	296.847	298.306	299.471	1,171(7)	2.674
KCl	295.590	296.461	298.266	299.141	873(7)	3.146
KBr	295.620	296.379	298.287	299.041	757(7)	3.300
KI	295.570	296.236	298.243	298.897	660(7)	3.533
$KMnF_3$		296.646		299.214		2.960

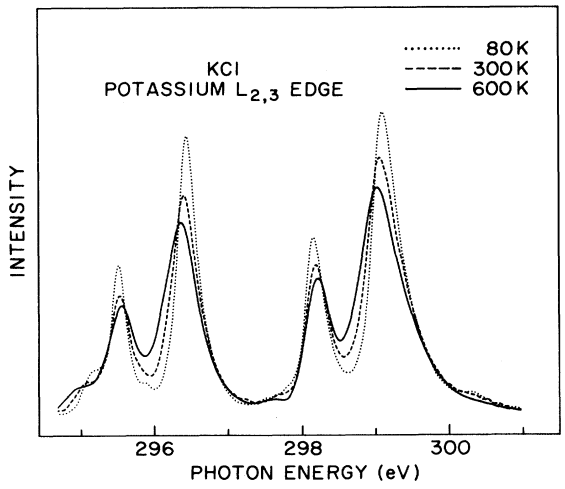

FIG. 3. Potassium $L_{2,3}$ edge photoabsorption spectra of KCl taken at 80 (dotted line), 300 (dashed line), and 600 K (solid line). The energy scale refers to the 300-K spectrum. The 80- and 600-K spectra have been arbitrarily shifted to help visualizing the changes.

the $2p^{-1}3d$ core exciton is different for each instantaneous arrangement of the atoms. The measured line shape, therefore, results from averaging over all the excitation energies, each being determined by the crystal-field splitting of a particular atomic configuration. The strong dependence of this splitting on lattice size is also the cause of the observed temperature induced linewidth broadening being much larger than values comparable to changes in kT. This can be directly seen using Eq. (2) to derive

$$\frac{\delta\Delta}{\Delta}=5\frac{\delta a_1}{a_1}=5\frac{\delta T}{T+a_{10}/\alpha}\ , \tag{4}$$

where α and a_{10} are, respectively, the coefficient of linear expansion and the intercept of the a_1-versus-T linear relation at $T=0$ K.[10] This relation demonstrates that the relative variations of temperature and lattice size induce an $\sim$5-times-larger relative change of the splitting Δ. Our measured Δ values and the independently known values of the KCl a_1's at the respective temperatures are in good quantitative agreement with Eq. (4). Finally, the magnitude of these broadenings, being larger than that of the peak shifts, is consistent with temperature-induced variations of atomic relative root-mean-square displacements, being typically much larger than the static thermal expansion of the lattice.

The capability of the $10Dq$ theory in explaining the KCl data can be further explored by considering again the relation between the logarithm of Δ and the logarithm of a_1 at the different temperatures. The values taken from Table III(a) are shown as open circles in Fig. 2. In this distance range the slope is steeper than the theoretical value of -5; it is also in clear contrast with the trend observed among KF, KCl, KBr, and KI. The different behavior of the data points in Fig. 2 can be reconciled with the predictions of the $10Dq$ theory by allowing q, and consequently the quantum average $\langle r^4\rangle_{3d}$, to depend on halide atom and lattice size. The value of $\langle r^4\rangle_{3d}$ for the various potassium halides and for KCl at different temperatures can be calculated using the following expression, which was derived from Eqs. (2) and (3):

$$\langle r^4\rangle_{3d}=0.587\frac{\Delta a_1^5}{e^2}\ . \tag{5}$$

Using the experimental values of Δ and the corresponding values for a_1, we obtain the quantity $r=(\langle r^4\rangle_{3d})^{1/4}$. This quantity is obviously larger than the average radius $\langle r\rangle_{3d}$ of the potassium $3d$ orbitals. It can be shown that $\langle r\rangle_{3d}$ is proportional to r, and, in the case of an unscreened Coulomb potential, it can be directly calculated using the relation $\langle r\rangle_{3d}=0.831r$.[11] The r, $\langle r\rangle_{3d}$, and a_1 values are summarized in Table IV, together with the static and optical dielectric constants $\epsilon_1(0)$ and $\epsilon_1(\infty)$. We note that indeed the potassium $3d$ orbitals are considerably affected by both halide atom and lattice size. Most

TABLE III. (a) Summary of the photoabsorption energies of peaks A, B, A', and B' in KCl at different temperatures. The Δ values and the corresponding a_1's are also listed. Experimental accuracy and precision are the same as in Table II. (b) Full widths at half maximum of peaks A, B, A', and B' in KCl, at different temperatures. The 600-K values for peaks A and A' are not shown because their determination is affected by the overlap with the stronger peaks B and B'. See Fig. 3.

(a)

T (K)	A (eV)	B (eV)	A' (eV)	B' (eV)	Δ (meV)	a_1 (Å)
80	295.557	296.490	298.231	299.164	933(7)	3.123
300	295.590	296.461	298.266	299.141	873(7)	3.146
600	295.663	296.473	298.328	299.130	806(7)	3.185

(b)

T (K)	A (meV)	B (meV)	A' (meV)	B' (meV)
80	256(10)	320(10)	333(10)	461(10)
300	363(10)	434(10)	399(10)	585(10)
600		561(10)		712(10)

TABLE IV. r, $\langle r\rangle_{3d}$, a_1, $\epsilon_1(0)$, $\epsilon_1(\infty)$, and $\langle r\rangle_{3d,\mathrm{sc}}$ values for different potassium halides and for KCl at different temperatures (Refs. 11 and 12).

		r (Å)	$\langle r\rangle_{3d}$ (Å)	a_1 (Å)	$\epsilon_1(0)$	$\epsilon_1(\infty)$	$\langle r\rangle_{3d,\mathrm{sc}}$ (Å)
KF	(300 K)	1.598	1.328	2.674	5.46	1.85	1.549
KCl	(300 K)	1.819	1.512	3.146	4.84	2.19	1.839
KBr	(300 K)	1.864	1.549	3.300	4.90	2.34	1.916
KI	(300 K)	1.962	1.630	3.533	5.10	2.62	2.074
KCl	(80 K)	1.834	1.523	3.123	(4.94)[a]	(2.24)[a]	1.863
KCl	(300 K)	1.819	1.512	3.146	4.84	2.19	1.839
KCl	(600 K)	1.811	1.505	3.185	(4.66)[a]	(2.11)[a]	1.814

[a]The KCl values in parentheses are calculated using the experimental value $\beta=-0.93$ and the relation $\epsilon_1=\epsilon_{10}[1+\beta(a_1-a_{10})]$, where ϵ_{10} and a_{10} are the 300-K values (Ref. 10). We assumed that β, measured for $\epsilon_1(0)$, also applies to $\epsilon_1(\infty)$.

interestingly, we observe that the different behaviors of the data points in Fig. 2 arise from the fact that the relation between $\langle r\rangle_{3d}$ and a_1 for the different potassium halides is reversed compared to that for KCl at different temperatures. This behavior can be understood by considering the relation between $\langle r\rangle_{3d}$ and the dielectric screening of the $2p^{-1}3d$ core exciton. The Coulomb attractive potential between the $2p$ core hole and the $3d$ electron is reduced by the screening of the electrons in the surrounding ions. The weakening of this attractive potential, which is macroscopically described by the magnitude of the dielectric constant, affects the spatial extent of the $3d$ orbitals. For higher dielectric constants, i.e., better screening, the spatial extent is larger, i.e., $\langle r\rangle_{3d}$ is also larger. Using the measured dielectric constants listed in Table IV,[12,13] we observe that $\langle r\rangle_{3d}$ and the static dielectric constant $\epsilon_1(0)$ have the same trend from sample to sample, except in the cases of KF at 300 K and KCl at 80 K. If instead of $\epsilon_1(0)$ we consider the optical dielectric constant $\epsilon_1(\infty)$, this discrepancy is removed. The relations between $\langle r\rangle_{3d}$ and the dielectric constants $\epsilon_1(0)$ and $\epsilon_1(\infty)$ are illustrated in Fig. 4. We see that the dependence of $\langle r\rangle_{3d}$ on $\epsilon_1(\infty)$ is not only monotonic, but also quite linear, in agreement with the very simple model of a hydrogenoid atom.[14] We should emphasize, however, that this linearity is found only when considering the *optical* dielectric constant, $\epsilon_1(\infty)$. This result, indicating that only $\epsilon_1(\infty)$ is appropriate to describe both the screening of the core hole and the $3d$-orbital spatial extent, is consistent with the short time scale of the photoabsorption process.

This dielectric screening of the $2p$ core hole has further implications in the use of the $10Dq$ theoretical model. The calculated values for q and for $\langle r\rangle_{3d}$ were derived using D values obtained from the unscreened Coulomb potential of Eq. (1). We suggest that to approximately take into account the dynamical screening effect, one should use the optical dielectric constant $\epsilon_1(\infty)$ to screen the crystal-field potential. The D values are then modified as

$$D_{\mathrm{sc}}=\frac{D}{\epsilon_1(\infty)}\ , \tag{6}$$

and the modified values for q and $\langle r\rangle_{3d}$ can then be calculated. For completeness, the new values $\langle r\rangle_{3d,\mathrm{sc}}=[\epsilon_1(\infty)]^{1/4}\langle r\rangle_{3d}$ are listed in the last column of Table IV. These new values for the $3d$ orbital spatial extent are slightly larger than the unscreened values. They are, however, still much smaller then the first-neighbor distance a_1, contrary to what is well known from the potassium halide ground-state band-structure calculation,[15] where the potassium $3d$ orbitals are delocalized, and form bands with wide energy dispersion. This demonstrates that the $3d$ orbitals are collapsed toward the $2p$ core hole and confirm the core-excitonic character of the $2p^{-1}3d$ transition. The attraction of the $3d$ orbitals toward the $2p$ hole is also responsible for the Δ values being smaller then those derived from $3p^{-1}3d$ shallow core excitons.[4] In fact, in the present case, the stronger attraction of the more localized $2p$ hole reduces more effectively the size of the $3d$ orbitals, and this, by reducing q reduces the value of Δ.

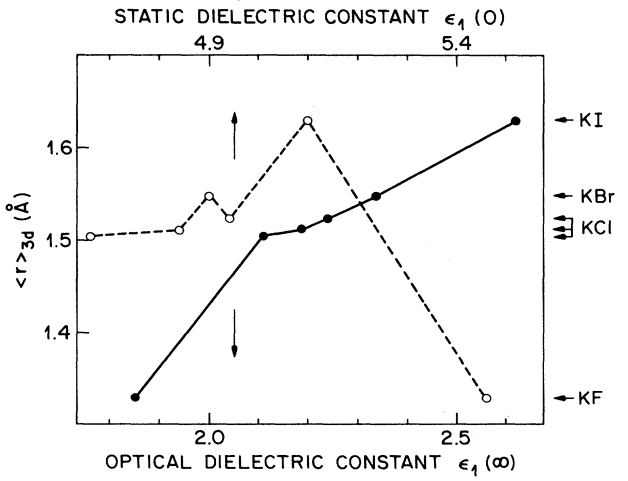

FIG. 4. Relation between the potassium $3d$ orbitals spatial extent $\langle r\rangle_{3d}$ and the dielectric constants $\epsilon_1(0)$ and $\epsilon_1(\infty)$. The data points are taken from Table IV. The $3d$-orbital spatial extent of each sample is indicated by the arrow on the right-hand vertical axis. The solid and dashed lines are a guide to the eye.

TABLE V. Unsplit values for the $2p^{-1}3d$ transitions E and E' and the corresponding optical dielectric constant $\epsilon_1(\infty)$, for different potassium halides and for KCl at different temperatures. The E and E' values are calculated according to Eq. (7) using the numbers listed in Tables II and III.

		E (eV)	E' (eV)	$\epsilon_1(\infty)$
KF	(300 K)	296.142	298.771	1.85
KCl	(300 K)	295.938	298.615	2.19
KBr	(300 K)	295.924	298.589	2.34
KI	(300 K)	295.837	298.504	2.62
KCl	(80 K)	295.930	298.604	2.24
KCl	(300 K)	295.938	298.615	2.19
KCl	(600 K)	295.987	298.648	2.11

Finally, the dynamical screening effect is also found to modify the photoabsorption energy of peaks A, B, A', and B' in these crystals. Using the energy positions of the peaks A and B (A' and B') listed in Tables II and III, we can calculate the unsplit energy position of the $2p^{-1}3d$ core exciton. According to the $10Dq$ model this quantity $E(E')$ is given by

$$E=\frac{6A+4B}{10} . \tag{7}$$

The values for E and E' are given in Table V together with the optical dielectric constant $\epsilon_1(\infty)$. According to the $10Dq$ theory the quantities E and E', representing the transition energies from the $2p$ level to the unsplit $3d$ level, should be unaffected by the crystal-field potential.[2] As shown in Table V, there is a slight variation in the values of E and E' among different potassium halides and KCl at different temperatures. The observed variation can be related again to the optical dielectric constant $\epsilon_1(\infty)$. A monotonic increase in E and E' is observed for decreasing values of $\epsilon_1(\infty)$. This behavior is consistent with the fact that a less efficient dynamical screening of the core-hole, i.e., a smaller $\epsilon_1(\infty)$, is responsible for an increase in the energy required for the excitation of the $2p^{-1}3d$ core exciton.

IV. CONCLUSIONS

In conclusion, we used high-resolution soft-x-ray spectroscopy to study the crystal-field splitting of core excitons in ionic crystal. We applied the simple $10Dq$ theory to explain the dependence of crystal-field splitting on charge arrangements, thermal expansion, and atomic vibrational motion. A procedure for measuring the size of the core exciton was presented. The use of it allowed for studying the correlation between the orbital spatial extent of the excited electron and the dynamical screening of the core hole.

ACKNOWLEDGMENTS

We acknowledge P. H. Citrin for stimulating discussions and G. Meigs for valuable technical assistance. This work was done at the National Synchrotron Light Source, which is supported by the U.S. Department of Energy under Contract No. DE-AC02-76CH00016.

[1]H. Bethe, Ann. Phys. (Leipzig) **3**, 133 (1929); J. H. Van Vleck, J. Chem. Phys. **7**, 72 (1939).

[2]S. Sugano, Y. Tanabe, and H. Kamimura, *Multiplets of Transition-Metal Ions in Crystals* (Academic, New York, 1970), and references therein.

[3]F. C. Brown, in *Synchrotron Radiation Research,* edited by S. Doniach and H. Winick (Plenum, New York, 1980), and references therein.

[4]M. Skibowski, G. Sprüssel, and V. Saile, Appl. Opt. **199**, 3978 (1980).

[5]A. A. Maiste, R. E. Ruus, and M. A. Elango, Zh. Eskp. Teor. Fiz. **79**, 1671 (1980).

[6]M. Yanagihara, H. Maezawa, T. Sasaki, and Y. Iguchi, J. Phys. Soc. Jpn. **54**, 3628 (1985).

[7]C. T. Chen, Nucl. Instrum. Methods A **256**, 595 (1987).

[8]C. T. Chen and F. Sette, Rev. Sci. Instrum. (to be published).

[9]Similar conclusions were reached in the calculated atomic-absorption spectra with O_h symmetry. J. Zaanen, G. A. Sawatzky, J. Fink, W. Speier, and J. C. Fuggle, Phys. Rev. B **32**, 4905 (1984).

[10]Y. S. Touloukian, R. K. Kirby, R. E. Taylor, and T. Y. R. Lee, *Thermophysical Properties of Matter* (IFI/Plenum, New York, 1977), Vol. 13. For KCl, $\delta a_1/a_1$ with respect to the 300-K value is -0.723% at 80 K and $+1.233\%$ at 600 K. An approximate value for the quantity a_{10}/α is 340 K.

[11]A. Messiah, Quantum Mechanics (North-Holland, New York, 1976), Vol. I, p. 484.

[12]M. P. Tosi, in *Solid State Physics,* edited by F. Seitz and D. Turnbull (Academic, New York, 1964), Vol. 16, p. 1.

[13]J. A. Van Vechten, Phys. Rev. **182**, 891 (1969).

[14]N. W. Ashcroft and N. D. Mermin, *Solid State Physics* (Holt, Rinehart and Winston, New York, 1976), p. 579.

[15]F. Bassani and G. Pastori Parravincini, *Electronic States and Optical Transitions in Solids* (Pergamon, New York, 1975), pp. 142–148 and references therein.